Morphology, Projection Pattern, and Neurochemical Identity of Cajal's "Centrifugal Neurons": The Cells of Origin of the Tectoventrogeniculate Pathway in Pigeon (*Columba livia*) and Chicken (*Gallus gallus*)

Tomas Vega-Zuniga,[1]* Jorge Mpodozis,[2] Harvey J. Karten,[3] Gonzalo Marín,[2,4] Sarah Hain,[1] and Harald Luksch[1]

[1]Lehrstuhl für Zoologie, Technische Universität München, Freising-Weihenstephan, Germany
[2]Laboratorio de Neurobiología y Biología del Conocer, Departamento de Biología, Facultad de Ciencias, Universidad de Chile, Santiago de Chile, Chile
[3]Department of Neurosciences, School of Medicine, University of California San Diego, La Jolla, California, USA
[4]Facultad de Medicina, Universidad Finis Terrae, Santiago de Chile, Chile

ABSTRACT

The nucleus geniculatus lateralis pars ventralis (GLv) is a prominent retinal target in all amniotes. In birds, it is in receipt of a dense and topographically organized retinal projection. The GLv is also the target of substantial and topographically organized projections from the optic tectum and the visual wulst (hyperpallium). Tectal and retinal afferents terminate homotopically within the external GLv-neuropil. Efferents from the GLv follow a descending course through the tegmentum and can be traced into the medial pontine nucleus. At present, the cells of origin of the Tecto-GLv projection are only partially described. Here we characterized the laminar location, morphology, projection pattern, and neurochemical identity of these cells by means of neural tracer injections and intracellular fillings in slice preparations and extracellular tracer injections in vivo. The Tecto-GLv projection arises from a distinct subset of layer 10 bipolar neurons, whose apical dendrites show a complex transverse arborization at the level of layer 7. Axons of these bipolar cells arise from the apical dendrites and follow a course through the optic tract to finally form very fine and restricted terminal endings inside the GLv-neuropil. Double-label experiments showed that these bipolar cells were choline acetyltransferase (ChAT)-immunoreactive. Our results strongly suggest that Tecto-GLv neurons form a pathway by which integrated tectal activity rapidly feeds back to the GLv and exerts a focal cholinergic modulation of incoming retinal inputs. J. Comp. Neurol. 522:2377–2396, 2014.

INDEXING TERMS: optic tectum; GLv; slice; vine-neuron; ChAT; birds

The optic tectum (TeO), corresponding to the superficial portion of the mammalian superior colliculus (SC), is a multi-laminar structure located in the roof of the mesencephalon. In birds it is composed of 15 layers, each containing layer-specific cell populations (Ramón y Cajal, 1995). The avian tectum is in receipt of the majority of the retinal axons (Mpodozis et al., 1995; Karten et al., 1997), which terminate differentially into five specific layers within the superficial retino-recipient zone (Hayes and Webster, 1975; Angaut and Repérant, 1976; Ramón y Cajal, 1995). The TeO also receives afferents from several other sources, such as the ventral lateral thalamus (VLT), the tectal gray (GT), the isthmic nuclei pars parvocellularis (Ipc), pars magnocellularis (Imc) and pars semilunaris (SLu), the visual wulst (hyperpallium), and the nucleus spiriformis lateralis (SPL), each exhibiting a particular pattern of arborization within specific tectal layers. In addition, the TeO is

This article was published online on 19 April 2014. A production error was subsequently identified. This notice is included in the online version to indicate that it has been corrected on 26 April 2014.

Additional Supporting Information may be found in the online version of this article.

Grant sponsor: Fondo Nacional de Desarrollo Científico y Tecnológico; Grant numbers: 1110281, 1120124, 1080220.

*Correspondence to: Dr. Tomas Vega-Zuniga, Lehrstuhl für Zoologie, Technische Universität München, Liesel-Beckmann Str. 04, 85354 Freising, Germany. E-mail: tomas.vega-zuniga@tum.de

Received October 28, 2013; Revised January 13, 2014;
Accepted January 13, 2014.
DOI 10.1002/cne.23539
Published online January 17, 2014 in Wiley Online Library (wileyonlinelibrary.com)

the locus of origin of several efferent ascending and descending visual pathways that arise from different layer-specific cell populations (Vanegas, 1984; Wylie et al., 2009). The tectal ganglion cells located in layer 13 are the source of the ascending tectofugal pathway (TeO → nucleus Rotundus → Entopallium), which is a main visual pathway in amniotes, including mammals (Benowitz and Karten, 1976; Reiner, 1994; Luksch et al., 1998; Major et al., 2000; Dávila et al., 2002). Deep and intermediate tectal layers are also the origin of two major descending projections to the hindbrain: the crossed tectobulbar pathway (CTB) and the ipsilateral tectoreticular-tectopontine pathway (ITP) (Reiner and Karten, 1982; Hellmann et al., 2004). Other significant efferent projections arise from the intermediate layers and proceed to several thalamic and tegmental targets, such as the isthmic nuclei pars magnocellularis (Imc), parvocellularis (Ipc), and semilunaris (SLu), the isthmo optic nucleus (ION), the nucleus lentiformis mesencephali (LM), the tectal gray (GT), the thalamic OPT complex (homolog of the mammalian dorsal geniculate), the VLT, and the nucleus geniculatus lateralis pars ventralis (GLv) (Hunt and Künzle, 1976a; Crossland and Hughes, 1978; Crossland and Uchwat, 1979; Vanegas, 1984; Gamlin and Cohen, 1988; Wylie et al., 2009).

The GLv is one of the most prominent thalamic targets of retinal projections in all amniotes. In birds, the GLv is a distinctive structure nested in the optic tract in the ventrolateral diencephalon (Crossland and Uchwat, 1979). The avian GLv exhibits a characteristic cytoarchitecture composed of two main layers (as seen in Fig. 1): the lamina interna (GLv-li), which contains tightly packed somata of the projection cells, and the neuropil (GLv-ne) (Crossland and Uchwat, 1979; Guiloff et al., 1987; Tombol et al., 2004). The optic tectum is the main nonretinal source of GLv afferents. Retinal and tectal inputs end topographically and in homotopic correspondence inside the GLv-ne (Crossland and Uchwat, 1979). Other significant afferents originate from the visual wulst (homologous to the mammalian primary visual cortex) which produces a dense terminal field in the outer half of the GLv-ne, the tectal gray (GT), the nucleus lentiformis mesencephali pars magnocellularis (LMmc), and the ventrolateral thalamus (VLT) (Karten et al., 1973; Crossland and Uchwat, 1979; Gamlin and Cohen, 1988). Projections from the GLv follow a descending course through the pretectum and tegmentum (Hu et al., 2004), to finally target the nucleus pontis medialis (Pm) (Marín et al., 2001).

The phylogenetic conservation of the GLv, together with its complex pattern of connections with the main structures of the visual system, suggests that this nucleus plays a fundamental role within the neural structures subserving vision. However, in spite of several suggestions found in the literature such as chromatic discrimination (Maturana and Varela, 1982), circadian rhythm (Harrington, 1997), optokinetic reflex (Gioanni et al., 1991), and visuomotor responses (Pateromichelakis, 1979; Guiloff, 1991), the role of the GLv in vision remains unclear. In this context, a detailed survey of the TeO-GLv projection is of interest, as it may clarify which of the many visual operations taking place in the optic tectum are functionally linked to the GLv.

Previous work (Hunt and Künzle, 1976a) has shown that the tectal cells projecting to the GLv are located in layer 10, and correspond to the cell type previously described by Ramón y Cajal (1995) as "centrifugal neurons." In addition, Medina and Reiner (1994) suggested that these cells could correspond to the choline acetyltransferase (ChAT)-immunoreactive neurons located in tectal layer 10. To delineate the functional contribution of this neuronal circuit to vision, the neuronal morphology, projection pattern, and neurochemical identity of these cells require further assessment.

In order to clarify these essential issues, we performed in vivo experiments in pigeons and in vitro experiments in chicken brain slices (containing the TeO-GLv connection). We show that the TeO-GLv projection is indeed topographic, and originates from a population of radially oriented bipolar neurons with fusiform perikarya located in tectal layer 10. Conspicuous morphological characteristics of these cells are dense dendritic ramifications in layer 7 and an axon ascending in a vine-like fashion towards the ventral thalamus. In addition, we found that these cells are indeed ChAT-positive, and therefore the tectal influence over GLv might be cholinergic in nature.

Abbreviations

A	Arcopallium
GLv	Nucleus geniculatus lateralis pars ventralis
GLv-li	Nucleus geniculatus lateralis pars ventralis – lamina interna
GLv-ne	Nucleus geniculatus lateralis pars ventralis – neuropil
GP	Globus pallidus
GT	Tectal gray
H	Hyperpallium
HL	Nucleus habenularis lateralis
HM	Nucleus habenularis medialis
Hp	Hippocampus
ION	Isthmo optic nucleus
Ipc	Nucleus isthmi pars parvo cellularis
L	Field L
LM	Nucleus lentiformis mesencephali
LSt	Lateral striatum
M	Mesopallium
NCC	Nidopallium caudocentrale
NCL	Nidopallium caudolaterale
NI	Nidopallium intermedium
ot	Optic tract
OV	Nucleus ovoidalis
Rt	Nucleus rotundus
SO	Stratum opticum
SPL	Nucleus spiriformis lateralis
TeO	Optic tectum

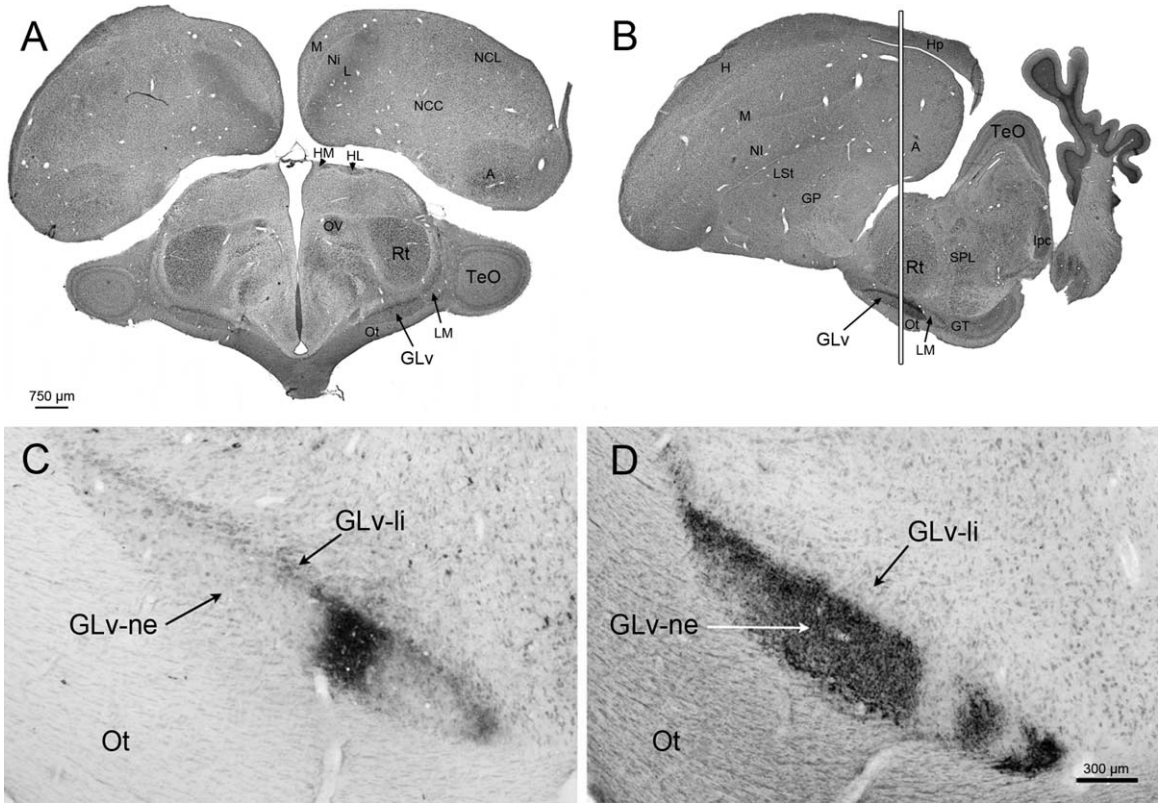

Figure 1. Tectal and retinal terminals in the GLv. **A:** Transverse plane of a Giemsa staining showing the position of the GLv in a dorsoventral orientation. **B:** Sagittal plane of the Giemsa staining showing the position of the GLv in a rostrocaudal orientation. White vertical line represent approximately the location of the transverse sections in C and D. **C:** Anterogradely labeled CTb-terminals in the GLv-ne after tectal injection into intermediate layers (injection site not shown). **D:** Labeled terminals in the Glv-ne after intraocular injection of CTb. Empty areas in the GLv-ne may be due to uneven distribution of CTb into the vitreal chamber of the eye. Tectal and retinal afferents are topographic and coexist in close apposition into the GLv-ne. Scale bar in A apply to B. Scale bar in D apply to C.

MATERIALS AND METHODS

Animals

Twelve adult feral pigeons *(Columba livia)* of either sex, obtained from an authorized local dealer, were used in the in vivo experiments. All surgical procedures used on these animals were approved by the University of Chile's Ethics Committee and conformed to National Institutes of Health guidelines on the ethical use of the animals.

In addition, 23 White Leghorn chick hatchlings (*Gallus gallus*; postnatal (P-1 until P-3) were used in the in vitro experiments. Fertilized eggs were obtained from local breeders (Hatchery Hoelzl, Moosburg, Germany) and incubated at 37°C and 70% humidity. All in vitro procedures were approved by the Munich Veterinary Animal Care Committee and conformed to National Institutes of Health guidelines on the ethical use of the animals. All efforts were made to minimize both the suffering and the number of animals used in these experiments.

In vivo extracellular injections

Injections of 3–10 nL of a 1% solution of cholera toxin subunit b (CTb) (List Labs, Campbell, CA) were performed in 10 pigeons. The targets of these injections were the eye chamber (two cases), the GLv (five cases), and the TeO (three cases). In two additional pigeons, an injection of 200 nL of a 3% solution of kainic acid (Sigma, St. Louis, MO) was placed unilaterally into the nucleus Ipc for immunohistochemical experiments (see ChAT Immunohistochemistry section).

Pigeons were anesthetized with a combination of ketamine (40 mg/kg) and xylazine (12 mg/kg) injected intramuscularly. A single dose usually proved satisfactory for the duration of the surgical procedure. If necessary, a supplementary dose of anesthetic was administered (ketamine 10 mg/kg and xylazine 3 mg/kg every 2 hours). Injections into the eye chamber were performed manually under a dissecting microscope using an insulin syringe (30G needle). Injections into the GLv, the Ipc, and the TeO were achieved by

stereotaxically (Karten and Hodos, 1967) lowering a micropipette filled with the CTb solution into the desired area. Once the target was reached, the tracer was injected applying pressure pulses using a picospritzer (Picospritzer II, General Valve, Fairfield, NJ). In order to enhance the accuracy of the injections, electrophysiological responses were monitored during the stereotaxic penetration. For a detailed review of these procedures, see Mpodozis et al. (1996).

After the injections the wounds were covered, the skin sutured, and treated with topical antibiotics. During the experiments the heart rate of the animals was continuously monitored and the body temperature was held at 40–42C° by means of a thermoregulated electric blanket. During surgery and recovery all wounds and pressure points were treated with a commercial ointment of 5% lidocaine.

After 5–9 days of survival, and 30 days in the cases with the kainic acid injection, the animals were deeply anesthetized with an overdose of a mixture of ketamine and xylazine and perfused via the aorta with 500–800 ml of 0.75% saline, followed by 1,000 ml of an ice-cold solution of 4% paraformaldehyde in 0.1 M phosphate buffer (PB, pH 7.4). After the perfusion, brains were excised, postfixed overnight in the paraformaldehyde solution, and then transferred for 2–3 days to a 30% sucrose solution (in 0.1 M PB) for cryoprotection. The brains were then mounted in the stereotaxic plane over the stage of a frozen sliding microtome and 30 μm sections were cut in the transverse plane.

In the cases with the CTb injection, sections were washed 30 minutes in 0.1 M phosphate-buffered saline (PBS, pH 7.4) and incubated in goat anti-CTb (1:15,000, List Labs) overnight at 4°C. The tissue was then processed using the avidin-biotin-peroxidase method (ABC Elite kit, Vector Labs, Burlingame, CA) in 0.3% Triton X-100 in PB for 1 hour. Sections were then washed in PBS and reacted in 0.025% diaminobenzidine (DAB, Sigma) and 0.3% hydrogen peroxide in PB for 10 minutes. The tissue was mounted on gelatinized slides, dehydrated, cleared, and coverslipped using Permount (Fisher Scientific, Fair Lawn, NJ). Previous control experiments using the same protocol but without CTb injection in the brain were performed. The results showed no labeling in the brain of pigeons (data not shown).

In vitro extracellular injections

Injections targeting the GLv and the TeO in the chicken were made using 12 nL of a 10% solution of dextran biotin (BDA 10,000 MW, Molecular Probes) or dextran Alexa Fluor 546 10% (10,000 MW, Invitrogen, Molecular Probes) dissolved in PB 0.1 M.

Chick hatchlings were deeply anesthetized with a mixture (3:1) of ketamine (50 mg/ml; Inresa Arzneimittel) and Rompun (2%; Bayer, Leverkusen, Germany) at 37.5 and 5 mg/kg, respectively, and subsequently decapitated. The skull was opened at the midsagittal line and the dorsal surface of the brain exposed. After removal, the brain was transferred into ice-cooled (4°C) sucrose-substituted Krebs solution (210 mM sucrose, 3 mM KCl (Sigma), 3 mM $MgCl_2 \cdot 6H_2O$, 23 mM $NaHCO_3$, 1.2 mM $NaH_2PO_4 \cdot 6H_2O$ (Laborbedarf-Vertrieb, Germany), 11 mM D+-glucose).

The forebrain and cerebellum were removed with cuts through the junction with the diencephalon and the cerebellar peduncles. The remaining parts of the brain were cut midsagittally into two hemispheres. The brain tissue was then embedded in agar at 48°C and rapidly cooled (1.5% agar in HEPES solution: 290 mM sucrose, 3 mM KCl, 3 mM $MgCl_2$, and 5 mM HEPES; Sigma). The optic tectum of each hemisphere was aligned in an oblique transverse plane. The hemispheres were cut into slices between 500–900 μm with a vibratome (VF 200 Microtome, Precisionary Instruments, CA, USA). Slices containing the TeO-GLv were placed in standard ACSF solution (120 mM NaCl, 3 mM KCl, 1 mM $MgCl_2 \cdot 6H_2O$, 23 mM $NaHCO_3$, 1.2 mM $NaH_2PO_4 \cdot 1H_2O$, 11 mM D+-glucose) and kept submerged in a chamber that was bubbled continuously with carbogen (95% oxygen, 5% CO_2) at room temperature for at least 30 minutes.

Pipettes were fabricated from borosilicate glass (GB100-8P, 0.58 × 1.00 × 80 mm; Science Products, Germany) with a one-stage microelectrode puller (Sutter Instrument, USA) to produce a tip opening ~30 μm. The electrodes were filled with mineral oil and attached to a Nanoliter 2000 injector (World Precision Instruments, USA). Electrodes were filled with dextran biotin 10% (BDA 10,000 MW, Molecular Probes) or dextran Alexa Fluor 546 10% (10,000 MW; Invitrogen, Molecular Probes) dissolved in PB 0.1 M.

Single slices were submerged in a chamber with carbogenated ACSF solution. Under microscopic control and using a microdrive (Maerzhaeuser, West Germany), injections of 13.8 nL tracer solution in three different positions along the GLv-ne were performed (medio-lateral axis).

After injecting, slices were incubated 4 hours in carbogenated ACSF solution to allow transport of the tracer.

Slices containing BDA backfills were fixed overnight in 4% paraformaldehyde in 0.1 M phosphate buffer (PFA/PB), transferred to 30% sucrose solution (in PB) for 2 hours, and cut to 60-μm sections with a cryotome (Kryostat 1720, Leitz, Germany). To visualize the filled

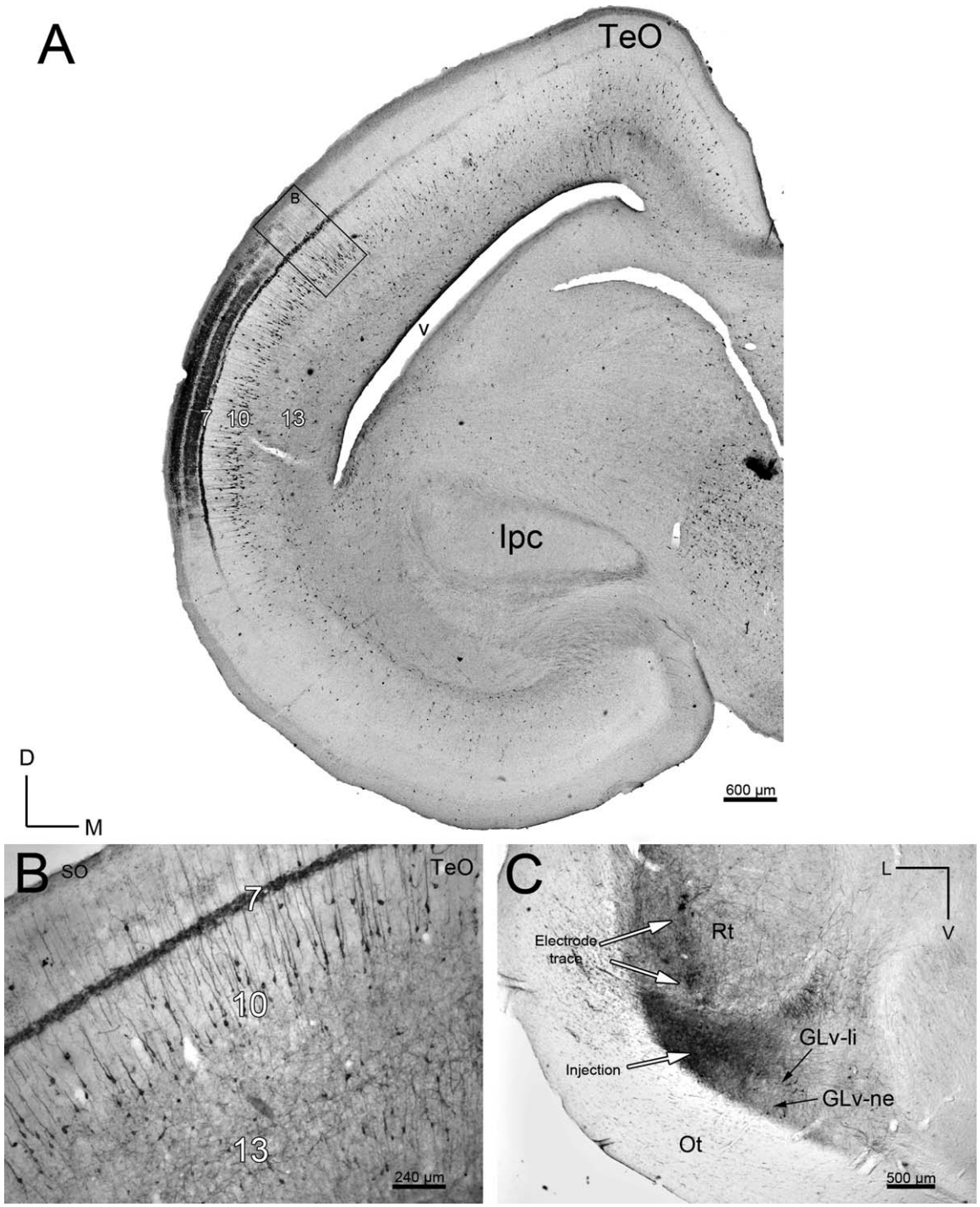

Figure 2. Retrograde tracing of the TeO-GLv projection in vivo. **A:** Retrograde CTb-labeling of cells located mainly in layer 10 of the TeO after a GLv injection. **B:** Higher magnification of the labeled cells located in layer 10 of the TeO. Note the heavily labeled processes in the layer 7. **C:** Corresponding injection site in the lateral GLv. Orientation in A is the same as B. V = ventral; L = lateral.

neurons, a heavy-metal-intensified DAB protocol was applied. Sections were first incubated in H_2O_2 solution (3% (wt/vol) H_2O_2) for 30 minutes to block endogenous peroxidase. After washing eight times (8 × 10 minutes) in PB 0.1 M until oxygen bubbles disappeared, sections were incubated in 0.1% (vol/vol) avidin-biotinylated horseradish peroxidase (HRP) complex (ABC Elite kit, Vector Labs, Burlingame, CA) solution containing 0.5% (vol/vol) Triton X-100 for 2 hours. Afterwards, samples were incubated in 0.026% diaminobenzidine Ni-Co with 0.03% H_2O_2 for 6 minutes. Sections were mounted onto gelatin-subbed slides, dehydrated in an ethanol series

ending in xylol, and coverslipped with DPX (Sigma-Aldrich, Germany).

In vitro intracellular filling

Intracellular fillings were performed in chicken slices. The target of this experiment was to randomly fill bipolar cells located in layer 10 of the TeO.

Electrodes were fabricated from borosilicate glass (GB150 F-8P, 0.86 × 1.50 × 80 mm, filament; Science products, Germany) with a two-stage microelectrode puller (DMZ Universal) to produce electrodes with a resistance of 60–80 MΩ. The electrodes were filled with a mixture of 3% biocytin (hydrochloride, Sigma-Aldrich) and 0.5% sulforhodamine 101 (Sigma-Aldrich) dissolved in 0.05 M Tris-buffer (pH 7.4) with 0.5 M KCl.

After incubation in Acridin Orange (10 mM, Sigma-Aldrich) for at least 20 minutes, single slices were transferred into a custom-built submerged slice chamber on a microscope stage that was continuously perfused with artificial cerebrospinal fluid (ACSF) solution (21/22°C); slices were stabilized with a U-shaped platinum holder.

Sharp electrodes were moved through the tissue using a micromanipulator (MWS-1A Narishige, Japan) under an epifluorescent microscope (NikonY-FL, Eclipse E600FN, Japan). Once a cell was penetrated, biocytin/rhodamine was injected into the cell with a positive current of 0.8 nA for 5 minutes. After a successful filling corroborated with rhodamine fluorescence, slices were incubated for 3 hours in carbogenated ACSF solution, then fixed overnight in 4% paraformaldehyde in 0.1 M phosphate buffer (PFA/PB), transferred to 30% sucrose solution (in PB) and cut into 50-μm slices with a cryotome (Kryostat 1720, Leitz, Germany).

To visualize the neurons filled with biocytin, a slightly different heavy-metal-intensified DAB protocol was applied. Sections were first incubated in H_2O_2 solution (3% (wt/vol) H_2O_2) for 30 minutes to block endogenous peroxidase. After washing 8 × 10 minutes in PB 0.1 M until oxygen bubbles disappear, slices were incubated in 0.5% (vol/vol) avidin-biotinylated HRP complex (ABC) solution containing 0.5% (vol/vol) Triton X-100 overnight. Afterwards, samples were incubated in 0.026% diaminobenzidine Ni-Co for 10 minutes. The chromogenic reaction was done adding H_2O_2 (final concentration 0.01%) for 60 seconds. Finally, sections were mounted onto gelatin-subbed slides, dehydrated, and coverslipped in DPX.

ChAT immunohistochemistry in vivo and in vitro

Choline acetyltransferase (ChAT) is a marker of cholinergic cells. The goat polyclonal anti-ChAT antibody (immunogen: human placental enzyme) has been well characterized and previously demonstrated to recognize 68–70-kDa bands in western blot analysis of brain extracts from rat and several species of fish that disappeared when the antibody was preincubated with human placental ChAT (Pérez et al., 2000; Gaillard et al., 2008; Hoshi et al., 2011; Sevigny et al., 2012).

ChAT immunohistochemistry was performed in both pigeon and chicken tissue. Pigeon sections were obtained from the animals that received a kainic acid injection into the lpc, according to the method described above. This procedure was performed in order to abolish the masking effect of the ChAT-li of the lpc neuron-paintbrushes in the medial and superficial layers of the TeO.

Chicken sections were from chicken slices containing either D-Alexa-546 backfills or without backfills. These slices were fixed overnight in 4% PFA in 0.1 M PB, transferred to 30% sucrose solution (in PB), and resectioned at 30 μm with the cryotome. Sections of both types were incubated with a primary antibody against anti-ChAT (goat, Chemicon, AB144P) 1:100 in a PBS 0.1 M solution containing 0.5% Triton X-100 and normal horse serum) overnight (4°C). After washing, sections of pigeon and chicken without backfills were incubated in secondary biotinylated antibody (rabbit antigoat 1:750, Vector Labs; BA-500) for 2 hours at room temperature. After washing in PB 0.1 M, sections were incubated in 0.1% (vol/vol) avidin-biotinylated HRP complex (ABC Elite kit, Vector Labs) solution containing 0.5% (vol/vol) Triton X-100 for 1 hour. Afterwards, samples were incubated in 0.026% diaminobenzidine Ni-Co with 0.03% H_2O_2 for 6 minutes. Sections were mounted onto gelatin-subbed slides, dehydrated, and coverslipped in DPX.

Chicken sections with backfills were incubated in secondary antibody Alexa 488 (A11055 donkey antigoat 1:200; Life Technologies, Molecular Probes) (Berger et al., 2010) for 2 hours at room temperature. Control sections were treated accordingly but the primary antibody was omitted. Sections were mounted onto gelatin-subbed slides and coverslipped with a custom made antifade mounting medium (propyl gallat 0.2%, Sigma-Aldrich; dimethyl sulfoxide [DMSO] 1%, Sigma-Aldrich; glycerol 90%; dissolved in PBS 1 M, pH 7.4). For a summary of the methods see table 1.

RESULTS

In vivo experiments

Anterograde tectal tracing.

Injections of CTb into the optic tectum resulted in the ipsilateral labeling of a well-delimited, dense plexus of axonal processes confined to discrete regions of the

GLv-ne (Fig. 1A). These tectal projections were topographically organized, as different injection sites into the optic tectum resulted in the labeling of fine axonal terminals in different locations within the GLv (data not shown). Tectal axonal terminals were of very fine caliber and spanned the whole dorsoventral extension of the GLv-ne, without noticeable invasion of the GLv-li. The distribution of the tectal terminals overlap fully with that of the more coarse retinal terminals, which also span densely through the whole extent of the GLv-ne until the limit with the GLv-li (Fig. 1B).

Injections of CTb into the optic tectum also resulted in the ipsilateral retrograde labeling of many cells within the IGL, the LMmc, and the VLT (data not shown). We were unable to find any indication of a similar substantial projection from the GLv upon the optic tectum. Only very rarely were retrograde CTb-labeled cells found in the GLv, even in cases with large tectal injections. These rare cells were located mostly in the GLv-li, with occasional ones appearing in the GLv-ne.

Retrograde GLv tracing.

Due to the peculiar shape of the GLv, we were unable to obtain restricted tracer injections either confined to the limits of the nucleus or resulting in a complete injection of the whole extent of the nucleus. The most consistent results (three cases) were achieved by injecting the central portion of the GLv, at the level of the central Rt (Fig. 2C). In these cases, only minor leakage to the Rt, the medially adjacent VSOD, the dorsally adjacent VLT, and the immediately ventral optic tract was observed. These injections consistently resulted in the ipsilateral retrograde labeling of a characteristic population of bipolar cells located in tectal layer 10 (Fig. 2A). These labeled cells had a very distinct morphology, featuring small fusiform somata and single apical and basal dendrites extending radially in opposite directions. The apical dendrite extended towards layer 2, and formed a conspicuous dense, transversely oriented specialization within the limits of layer 7 (Fig. 2B). The basal dendrite, of finer caliber, extended towards the deeper layers, and lacked evident specializations. In some instances it was possible to trace the axon of these cells arising from the apical dendrite and following an ascending course towards layer 1.

In vitro experiments

Tecto-thalamic connection.

To study the tecto-thalamic (TeO-GLv) connectivity with more detailed morphological features, oblique-transverse slices containing thalamus, pretectum and tectum (as seen in Fig. 3) were obtained. To ensure that the slices included the intact micro-circuitry between the TeO and the GLv, two localized extracellular injections of BDA-Alexa in the layers 9–10 of the ventral TeO were performed in four chickens (Fig. 4A). Tectal labeled neurons showed processes in both directions, apical and basal. The axons belonging to the labeled cells ascend to the superficial layers, proceed through the stratum opticum (SO) and optic tract (beneath GT and LM), and finally enter in an L-shape form into the GLv-ne, generating terminals in a topographic arrangement (Fig. 4B). The separation between the labeled terminals in GLv is 2.16 times smaller (107 μm) than the separation of the injections in the TeO (232 μm), indicating a scale reduction of the topographic map in the GLv.

In order to corroborate the existence of the described TeO-GLv projection in the slice, and to label the neurons generating this projection, localized

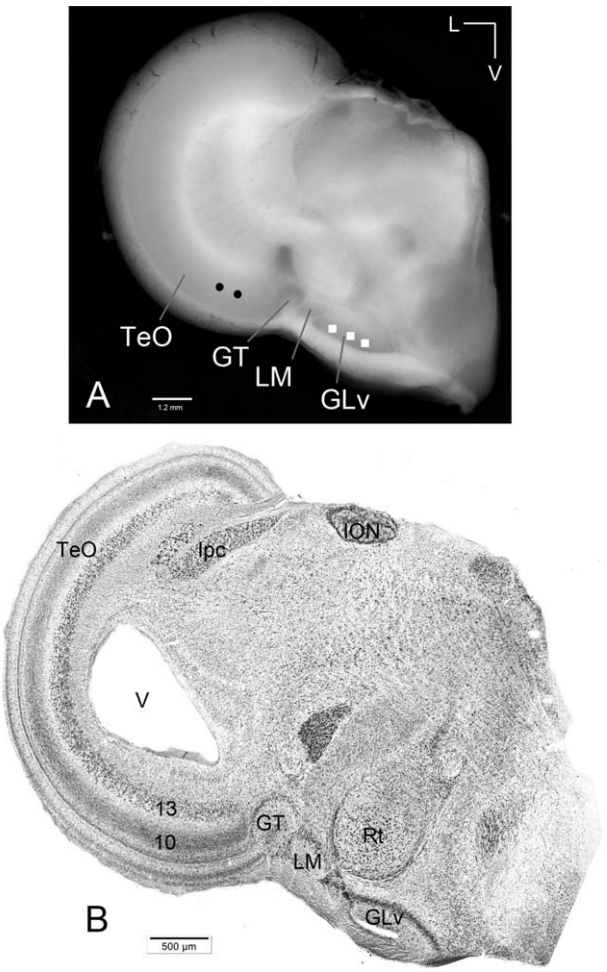

Figure 3. Chicken slice containing the TeO-GLv connection. **A:** Macrophotography of a typical 500-μm slice used in this study. Circles and squares mark the location of extracellular injections of dextran amines into the TeO and GLv (performed in each slice). **B:** Giemsa staining of a 60-μm section showing tectum, pretectum, and thalamus. V = ventricle. Orientation: M = medial; V = ventral.

extracellular BDA-injections in the GLv-ne were made in four chickens (Fig. 5B). Only radial neurons were retrogradely labeled. All these cells were localized to layer 10 of the TeO. The labeled tectal neurons were of striking similar morphology to the ones labeled after CTb injection into the GLv in vivo and showed a characteristic high-density process in layer 7 of the TeO (Fig. 5A). Retrograde labeled neurons were never observed in lateral and dorsal regions of the TeO, indicating that in our preparation only the connection between the ventral part of the TeO with the GLv remained intact.

Morphology and projection pattern of the vine-neurons.

Extracellular retrograde tracings in the GLv-ne and intracellular fillings in layer 10 of the TeO showed bipolar neurons with an oval-shaped soma located in the layer 10 of the TeO (Figs. 6, 8). The cells showed two primary dendritic branches: one rudimentary thin basal dendrite reaching into layer 13 (Fig. 6B), and a second thick apical dendritic trunk that extends through the superficial layers, giving rise to an extremely complex transverse arborization that spreads in layer 7 (Figs. 5A, 6, 8). Finally, the dendrite thins, branches out in layer 4, and continues towards layer 2 where it ends in a tripod-shaped pattern (Figs. 6E, 7). Strikingly, the axon splits from the apical dendritic trunk at the level of layer 9, ascending almost parallel, in a characteristic vine-like fashion (Figs. 6, 7, 10). Because of this conspicuous characteristic, we designated these cells "vine-neurons." At the level of layer 1 the axon turns 90° (as seen in Figs. 6E, 7, 10) towards the GLv passing through stratum

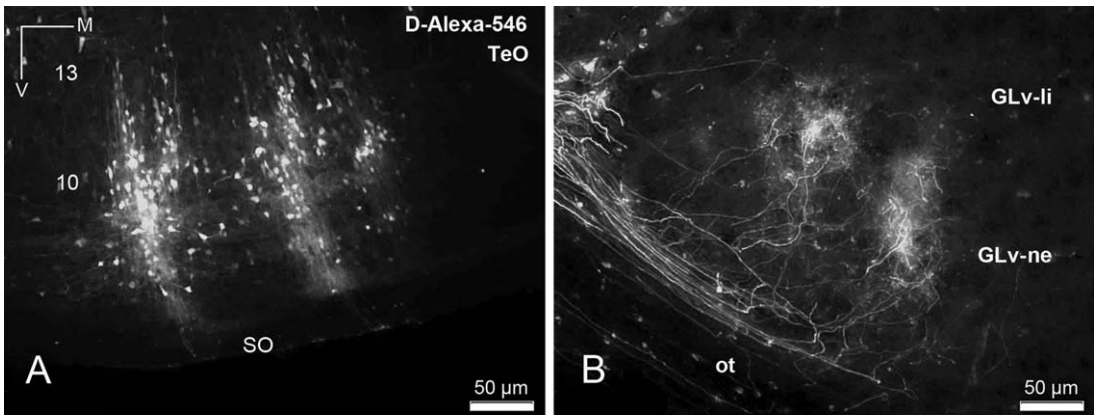

Figure 4. Anterograde tracing of the TeO-GLv projection. **A:** Two tectal injections of dextran-amine-alexa-546 (D-Alexa-546) in layer 9–10 of the TeO. **B:** Topographic terminals within the GLv-ne after the tectal injection. Orientation in B is the same as in A.

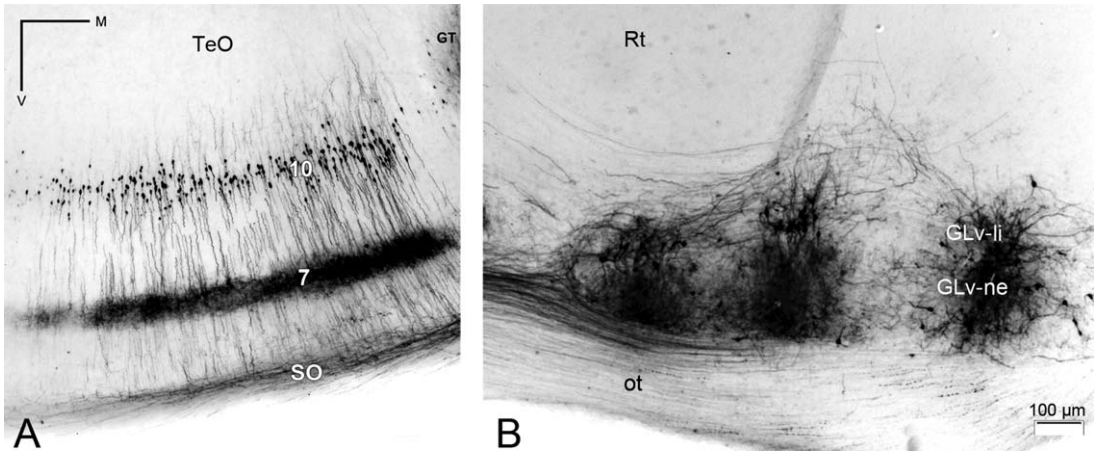

Figure 5. Retrograde tracing of the TeO-GLv projection. **A:** Composite image of five sections (separation between each section = 60 µm) of retrogradely labeled cells with somata located in layer 10 of the TeO after three injections of BDA in the GLv-ne. **B:** Extracellular injections of BDA into the GLv-ne. Note how cells in GLv-li are also heavy labeled. Scale bar in B apply to A.

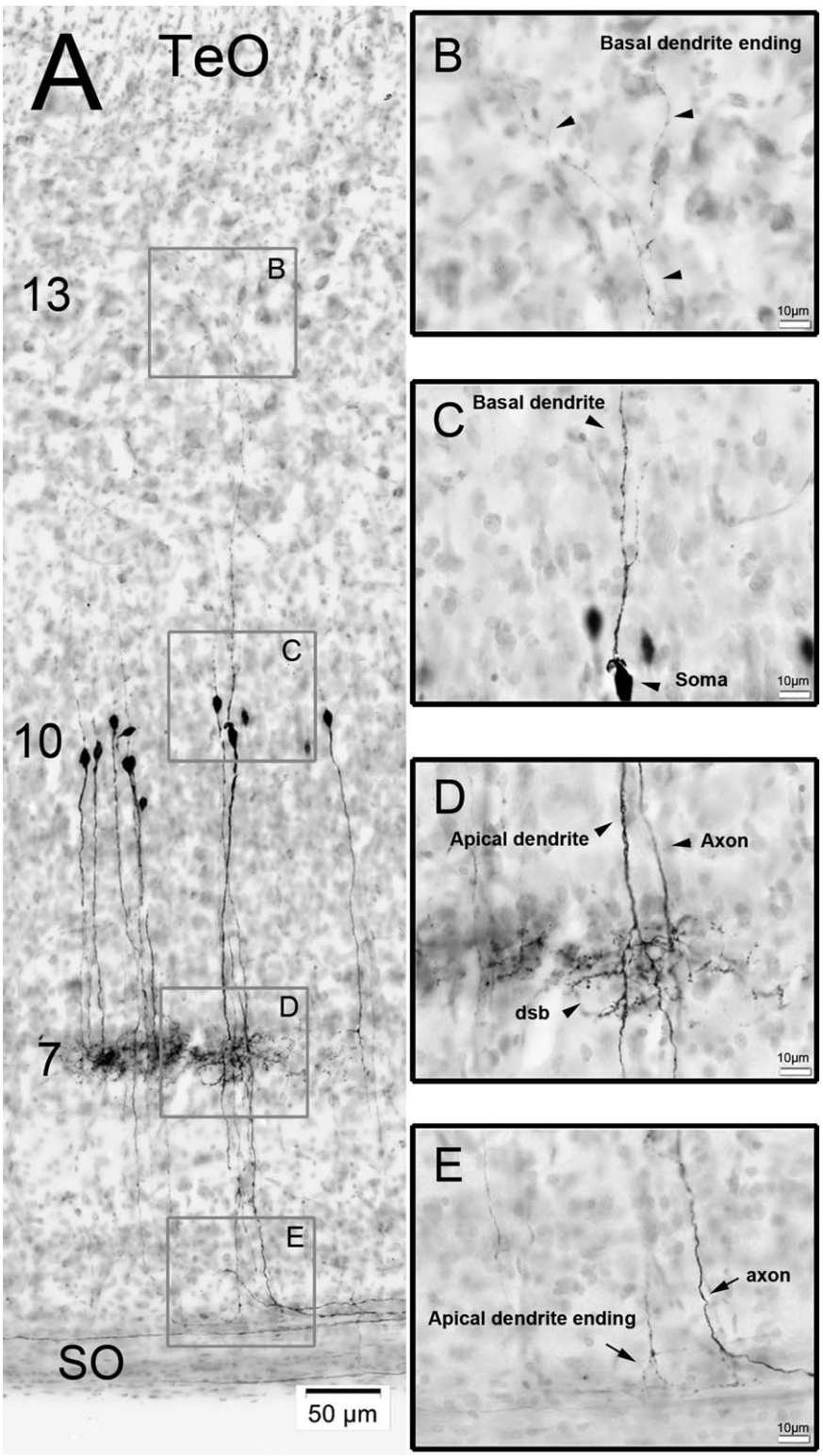

Figure 6. Retrograde labeling of cells in the TeO after BDA injections into GLv. **A:** Retrogradely labeled cells with Nissl counterstain. Basal dendrites extend until layer 13, somata are located in layer 10, dendritic side-branches lie in layer 7, and apical dendrites extend until layer 2 of the TeO. **B:** Inset showing the basal dendrite ending in layer 13 (black arrowheads). **C:** Inset showing the soma and the basal dendrite (black arrowheads). **D:** Inset showing the apical dendrite, the axon, and the dendritic side-branch (dsb) of a neuron (black arrowheads). **E:** Inset showing the apical dendrite ending and the axon of one vine-neuron. Note the 90° bending of the axons between layer 2 and SO.

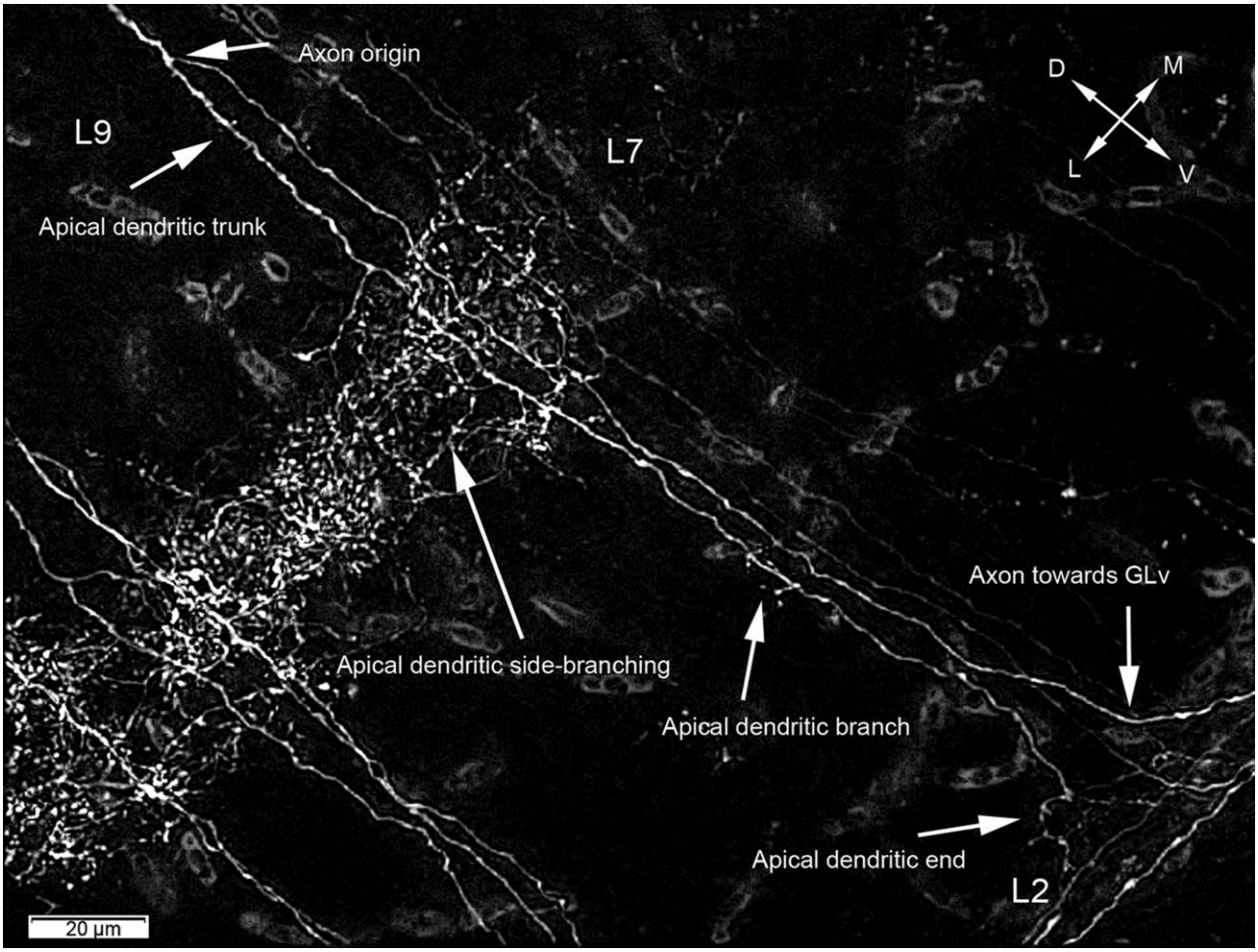

Figure 7. Deconvolution and extended focus projection of a retrogradely labeled cell in the TeO after GLv injection of D-Alexa-546. Retrograde labeling shows that the axon splits from the apical dendritic trunk at the level of layer 9. The apical dendrite side-branch massively in layer 7, continuing with a smaller branching in layer 4. Finally the apical dendrite ends in layer 2. Deconvolution used = Wiener. Orientation: L = lateral; V = ventral.

opticum (SO) and optic tract (Ot) subsequently. As shown in one complete intracellular filling, the terminal area is located in the GLv-ne (Fig. 9).

Neurochemical identity of the vine-neurons.

Previous reports of ChAT immunoreactivity in the TeO of birds (Sorenson et al., 1989; Medina and Reiner, 1994) consistently showed that the only ChAT-positive tectal cell bodies are located in layer 10, and correspond to a subpopulation of bipolar neurons whose apical dendrites seem to ramify in layer 7. In order to assess whether these cholinergic cells correspond to the vine-neurons, we first replicated these immunohistochemical studies in both pigeons (two cases) and chicks (two cases). Since in pigeons the afferent ChAT-positive axons from the nucleus lpc densely ramify across tectal layers, masking the intrinsic tectal ChAT immunoreactivity, we performed this study in tissue obtained from animals that had previously been subjected to a unilateral chemical ablation of the lpc using injections of kainic acid (see Materials and Methods and Fig. 11). Thus, the typical cholinergic "paintbrush endings" derived from the lpc were eliminated by the destruction of the corresponding region of the lpc.

In both species, anti-ChAT DAB-immunohistochemistry showed specific labeling of cells located in the layer 10 of the TeO, the lpc, and the nucleus nervi oculomotori (OM), among other structures (Figs. 11, 12A). The labeled neurons of layer 10 were distributed radially and closely resembled the size, morphology, and distribution of the vine-neurons described above (A-ChAT-488 soma size = 7.6 µm ± 0.80; A-546-dextran = 7.2 µm ± 0.6). Quantitative data ($n = 34$ cells) of the cell measurements were obtained from double-labeling experiments not shown here. (See also Figures 11C, 12B, 13B.)

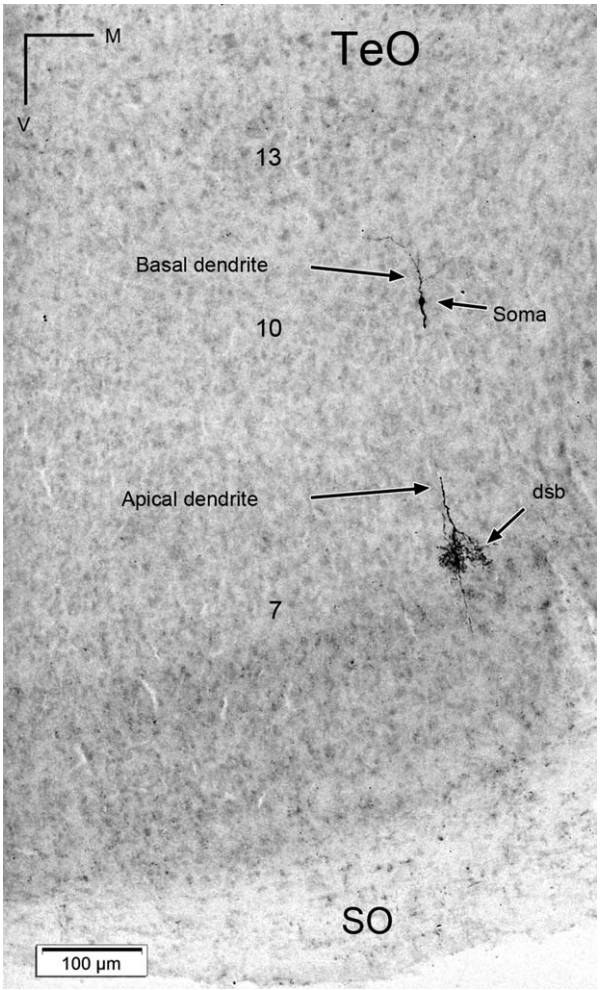

Figure 8. Intracellular filling of a vine-neuron with biocytin. The soma is located in layer 10 and the dendritic side-branch (dsb) in layer 7 of the TeO. Soma width = 5.0 µm; dendritic side-branch width = 66 µm.

Finally, to ensure that these anti-ChAT cells correspond to the tectal cells projecting to the GLv, double-labeling experiments were performed in three chickens. The results showed that all retrograde cells, marked after injections of BDA-Alexa in the GLv, positively colocalize with anti-ChAT immunoreactivity (Fig. 13), indicating a cholinergic neurochemical identity for the vine-neurons.

DISCUSSION

We were able to characterize the morphology, projection pattern, and neurochemical identity of the cells of origin of the TeO-GLv projection in two different avian species, pigeons and chickens, using complementary in vivo and in vitro approaches. Our data indicate that neurons located in layer 10 of the TeO, corresponding to Cajal's "centrifugal neurons," project in a topographic manner to the GLv, without giving collaterals to any of the pretectal structures near the axonal course. In addition, these cells are positive for ChAT immunoreactivity. Therefore, the TeO-GLv synapses are likely to be cholinergic in nature.

Slice limitations

Long and middle-range projections containing somata and terminals of the same neurons are rarely preserved in slice preparations, because they can easily course beyond the physical limits of the slice. Notwithstanding this, the results obtained in the in vivo experiments helped us to devise an unconventional plane of sectioning that resulted in slices containing, in its ventral aspect, the integrity of the TeO-GLv projection. Such slice preparation, together with the relatively rapid transport of dextran tracers (2 mm/h) (Fritzsch, 1993), allowed us to perform a detailed morphological analysis of this projection in the living slice. Specifically, we were able to label the TeO-GLv projecting cells with Golgi-like resolution (Reiner et al., 2000; Sebestény et al., 2002). The results obtained in the slice were fully consistent with those obtained in vivo, further confirming the validity of the in vitro approach used in this study.

Morphology and projection pattern of the vine-neurons

Tectal cells projecting to the GLv were first morphologically identified by Hunt and Künzle (1976b). They showed that these cells, a subpopulation of layer 10 bipolar cells featuring small fusiform somata, correspond to the ones previously described by Ramón y Cajal in 1891 as "centrifugal neurons" (Ramón y Cajal, 1995). The name "centrifugal" was given because Ramón y Cajal assumed that the conspicuous axons of these cells, which originated in layer 9 and left the tectum through the stratum opticum, would project to the retina. However, it has been repeatedly shown that in birds centrifugal neurons innervating the retina do not originate from the tectum, but from the isthmo-optic nucleus (ION) (Repérant et al., 2006). Thus, to avoid the confusion between the "true" centrifugal cells and the TeO-GLv ones, and given that these latter neurons show a conspicuous axon ascending in a vine-like fashion in the TeO, we suggest calling these cells "vine-neurons."

Our backfills confirmed that the somata of these cells are located in layer 10 of the TeO, mainly in layer 10b. This specific location suggests that vine-neurons may be positive for the transcription factor Brn3a, a specific marker for layer 10b, as Wang et al. (2006) showed for shepherd-crook neurons. Interestingly, in

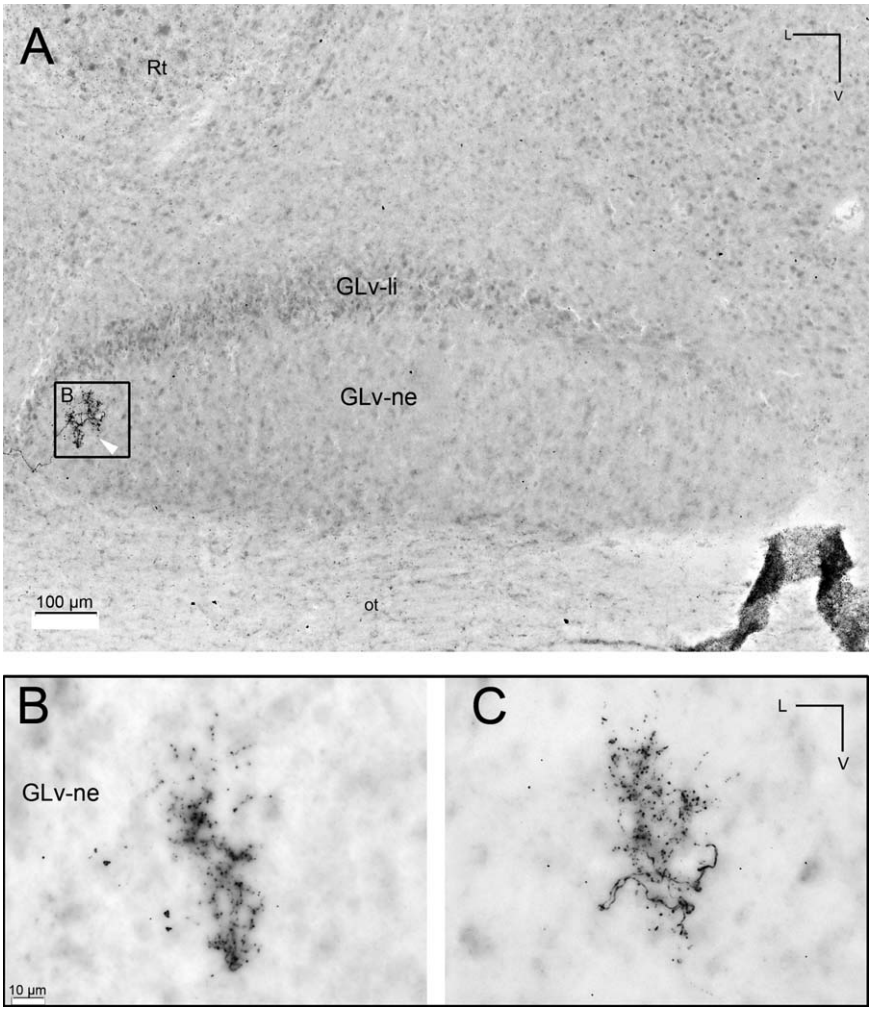

Figure 9. Intracellular filling showing a tectal terminal in the GLv-ne. **A:** Composite image of two contiguous 60-µm sections of the terminal of a vine-neuron in the lateral part of the GLv-ne. **B,C:** Inset showing the two sections where the terminal was observed. Scale bar in B apply to C.

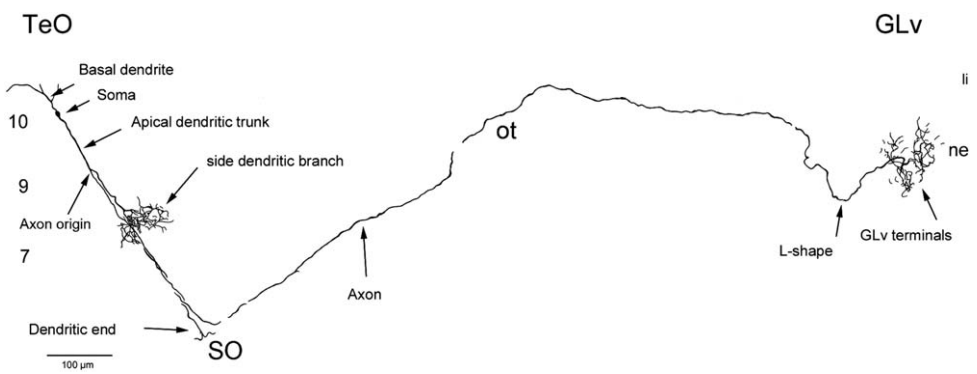

Figure 10. Reconstruction of an intracellularly filled vine-neuron with terminals in the GLv. Figure shows a complete filled neuron with biocytin. Basal dendrite does not reach layer 13 as previously shown probably because it extend beyond the limits of the slice. The axon runs through the upper limit of the SO and the Ot before entering the GLv. Note the L-shape form of the axon entrance into the GLv and the butterfly-shape of the terminal in GLv-ne. 10, 9, 7 = layers of the TeO.

Figure 11. Anti-ChAT immunohistochemistry in the pigeon. **A:** Overview of anti-ChAT-DAB labeling. Left side shows the intact Ipc nucleus and the characteristic ChAT-li of the paintbrush endings radially oriented in the TeO. Arrowheads on the right side outline the neurochemically ablated Ipc. **B:** Inset of the ventral part of the optic tectum showing mainly anti-ChAT-positive paintbrushes from the IPc neurons in layer 5. **C:** Anti-ChAT-positive somata located in layer 10 of the TeO are observed after chemical ablation of the Ipc nucleus. Note that the heavy staining previously observed in layer 5 (panel B) is no longer observed.

this latter study Brn3a labeled more cells than shepherd-crook neurons, suggesting the existence of another cell group in this sublayer.

In addition, our results corroborate that the horizontal branching expansion that these cells exhibit in layer 7 originates from the apical dendritic trunk (Figs. 6, 7) as Van Gehuchten suggested in 1892, and not from the axon as Ramón y Cajal pointed out in 1896 (Ramón y Cajal, 1995). These dendritic expansions may likely be the postsynaptic target of the subpopulation of retinal cells that give rise to the coarse, horizontally oriented terminals that densely cover layer 7. In addition, using the intracellular filling method we were able to label five vine-neurons; in two cases we could label the axon leaving the tectum, and in one case we could follow the whole trajectory of the axon as it enters and ramifies into the GLv-ne. As expected from the in vivo and in vitro results, this axonal terminal was very restricted and spanned through the dorso/ventral extent of the GLv-ne without reaching the GLv-li. We did not find any evidence of axon collaterals entering into the pretectal and thalamic structures located near the axonal course, such as LM, GT, and VLT.

Neurochemical identity of the vine-neurons

Immunohistochemical localization of different markers such as GABA, GAD, substance P, and ChAT has been extensively studied in the avian brain (Sorenson et al., 1989; Güntürkün and Karten, 1991; Bagnoli et al., 1992; Britto et al., 1992; Medina and Reiner, 1994; Veenman et al., 1994; Veenman and Reiner, 1994). Previous reports of ChAT immunoreactivity showed that in the TeO the only ChAT-positive cell population is a subset of layer 10 bipolar neurons featuring an apical dendrite that posses a characteristic expansion in layer 7. These previous studies have also shown that the GLv-ne is the only thalamic structure exhibiting a distinct plexus of cholinergic processes. Given these results, Medina and Reiner (1994) suggested that the source of such cholinergic processes were the tectal cells of layer 10.

We readily confirmed these previous observations and suggestions by means of anti-ChAT immune essays in pigeons and chickens. We found that the morphology and distribution of the ChAT-immunoreactive cells closely resemble that of the vine-neurons, indicating that both cell types are identical (Fig. 13). Our double-

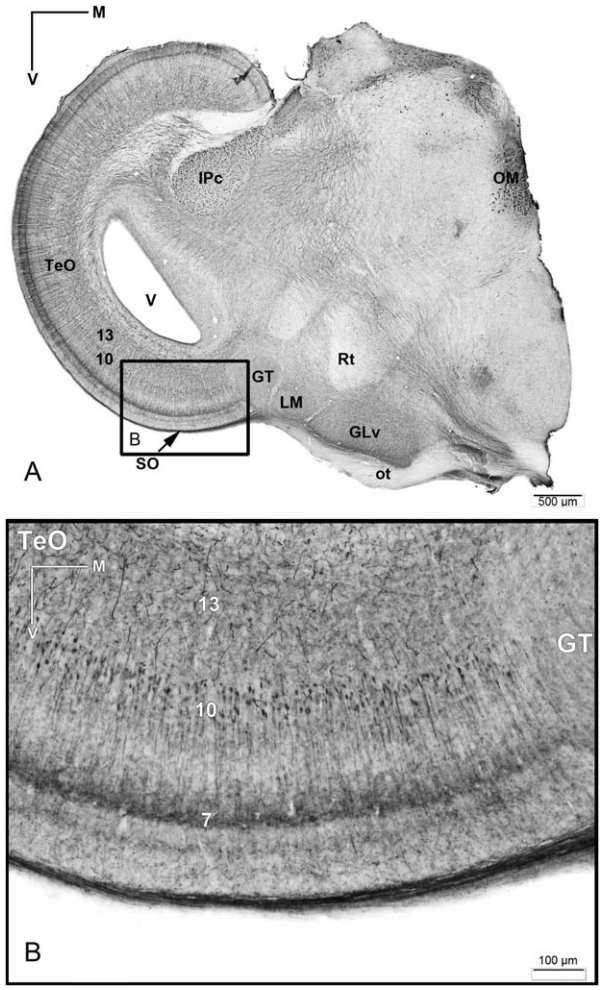

Figure 12. Anti-ChAT immunohistochemistry in chicken slice. **A:** Overview of diencephalic and mesencephalic structures showing anti-ChAT-DAB labeling. **B:** Inset of the ventral part of the optic tectum showing anti-ChAT-positive cells with the somata located in layer 10 of the TeO. Note that Layer 7 shows neurite immunoreactivity. V = ventricle.

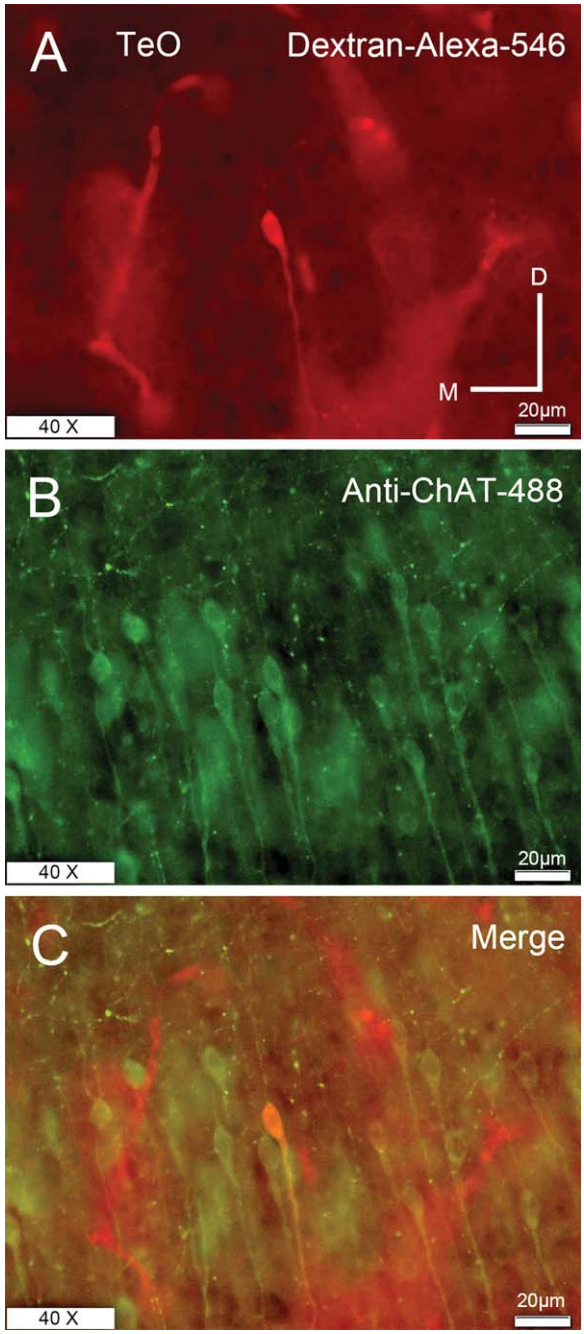

Figure 13. Double labeling experiments showing cells located in layer 10 of the TeO. **A:** Retrograde labeling of a vine-neuron with D-Alexa-546 located in layer 10 of the TeO after a GLv-ne injection. **B:** ChAT immunohistochemistry with Alexa-488 of the same section showing labeled cells in layer 10 of the TeO. **C:** Merge of both images showing ChAT labeling of the vine-neuron. All retrograde cells labeled with A-546-Dextran were positive for ChAT (data not shown). Orientation: M = medial; D = dorsal.

labeling experiments provide a direct confirmation of this identity, as we observed that all vine-neurons retrogradely labeled from the GLv were also ChAT-positive. We also observed that the intensity of cholinergic label in the GLv-ne appears greatly reduced after an excitotoxic lesion of the TeO (results not shown), confirming that the TeO is a source of cholinergic terminals upon the GLv. In addition, further physiological evidence shows that microstimulation in layer 10 of the TeO elicited cholinergic EPSP in the GLv (unpubl. results). Thus, our results strongly suggest that the TeO-GLv synapse is cholinergic in nature.

Contrary to what we show here, Hunt and Künzle (1976b) suggested that vine-neurons have a GABAergic identity. Such a conclusion was based on tracing studies using ^{3}H-GABA. However, what this method reveals is the uptake of GABA and not necessarily the neurochemical identity of these cells. In this regard, the literature shows the existence of GABA uptake in hippocampal cholinergic nerve endings (Bonanno and

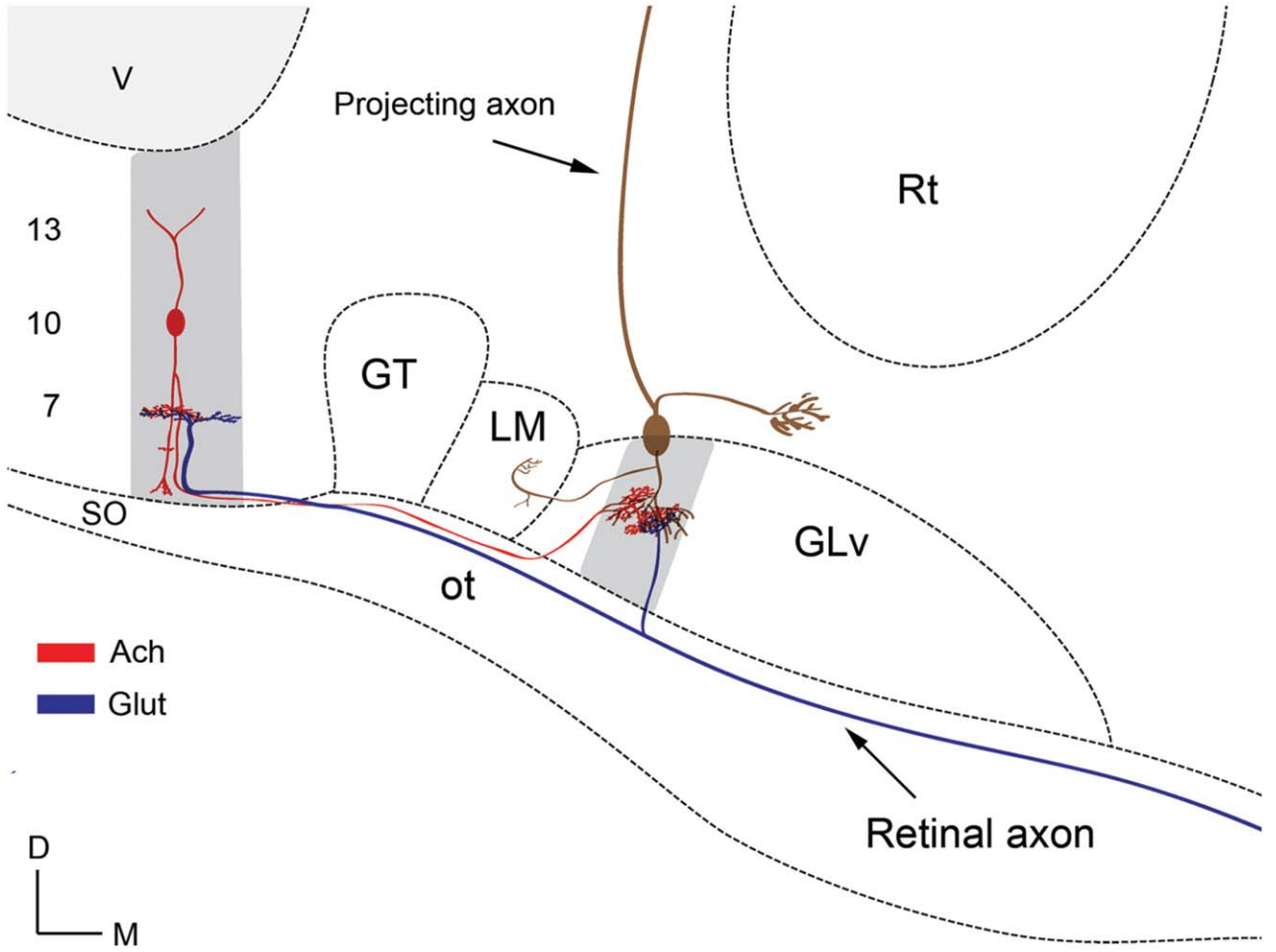

Figure 14. Schematic drawing of proposed neural circuitry of the TeO-GLv projection. Cholinergic vine-neuron located in layer 10 of the TeO (red) projects topographically onto a presumably GABAergic GLv projection cell (brown). Glutamatergic retinal input from a retinal ganglion cell ends in GLv and TeO (blue). The gray shadings indicate the activation of a specific locus in the TeO and the concurrent activation of an homotopic locus in the GLv. V = ventricle.

Raiteri, 1987). Moreover, in pigeon and chicken, first, the GLv-ne contains a dense plexus of GABA-containing processes, presumably caused by intrinsic GABAergic interneurons (Veenman et al., 1994; Tombol et al., 2004), and second, the GLv-li projection cells are presumably GABAergic (Sun et al., 2005). On the other hand, Veenman and Reiner (1994) and Sun et al. (2005) have shown that some cells located in layer 10 of the TeO are GABA-positive. In addition, previous experiments have shown the coexistence of ChAT-li and GABA in motor neurons in the hypoglossal nucleus in the rat (Davidoff and Schulze, 1988).

Hence, the presence of GABA in the vine-neurons (in the older studies) may likely be due to the reuptake of GABA at the axonal terminal in the GLv. However, further studies will be needed in order to rule out the GABAergic neurochemical identity of the vine-neurons.

GLv-TeO projection

Several reports suggest the existence of a reciprocal projection between the GLv and the TeO (Maturana and Varela, 1982; Guiloff et al., 1987). This alleged projection originates from a small population of cells and seems to be nontopographic (Hunt and Künzle, 1976a; Crossland and Uchwat, 1979; Wylie et al., 2009). In our in vivo experiments we found that the GLv cells retrogradely labeled from the TeO were always very scant, even after large tectal injections. Most of these cells were located in the GLv-li, but occasionally some of them were located in GLv-ne as well. In addition, the distribution of these rare labeled cells was very irregular, and showed no evidence of topographic arrangement. On the other hand, in our in vitro approach no retrograde labeled cells were found, probably due to the fact that the slice contains only part of the intact

TABLE 1.
Summary of the Methods Used

	Tectal injection	GLv injection	Intracellular filling	Anti-ChAT	Double labeling
In vivo pigeon	Yes CTb	Yes CTb	No	Yes with lesion in Ipc	No
In vitro chicken	Yes D-Alexa 488	Yes BDA, D-Alexa 488	Yes Biocytin	Yes	Yes D-Alexa 488 + ChAT-546

TeO-GLv connection. Thus, our results indicate that the population of GLv-tectum projecting cells is rather small and heterogeneous, and do not form a substantial organized projection as the TeO-GLv projection. This issue is relevant to clarify the TeO/GLv functional interactions.

Synaptic interactions in the retino-tecto-GLv network

Retinal fibers ending in the superficial layers (2–5 and 7) of the optic tectum are glutamatergic (Henke et al., 1976; Morino et al., 1991; Theiss et al., 1998; Atoji, 2011). At the same time, retino-recipient layers, including layer 7, express high levels of AMPA receptors Glu-R1 (Pires and Britto, 1997; Batista et al., 2002). We suggest that layer 7 labeling of Glu-R1 may correspond to the expression of these receptors in the dendritic side-branch of vine-neurons. If this is the case, retinal inputs may influence the activity of the vine-neurons. Following this notion, the axon that emerges from the apical dendritic trunk in layer 9 may generate a direct fast response (without necessarily an influence of the soma) that will arrive onto the GLv just a few milliseconds after the retinal input in both tectum and GLv. Furthermore, the apical dendrite of the vine-neurons proceeds beyond layer 7, crossing all tectal retino-recipient region until layer 2, thus possibly allowing for synaptic contacts with a myriad of different intrinsic or external sources, including other retinal subpopulations. Additionally, the basal dendrites of these cells, which extend until tectal layer 13, might interact with various types of processes present in these deep layers, such as the isthmic and arcopallial endings that terminate diffusely between layers 10–13. On the other hand, retinal terminals in tectal layer 7 also express high levels of nicotinic beta-2 receptors (Britto et al., 1992, 1994), suggesting a cholinergic presynaptic modulation of its glutamatergic release. Vine-neurons might be a possible candidate for modulation of these retinal terminals. In fact, dendritic release of several neurotransmitters has been widely shown to occur in the central nervous system of mammals (Cheramy et al., 1981; Isaacson, 2001; Ludwig and Pittman, 2003). Alternatively, the cholinergic paintbrush endings coming from the neurons of nucleus Ipc may enhance the retino-vine-neuron synapses at selected visually active loci. This is an interesting possibility that would link the activity of the retino-GLv projection with the presumed attentional function of the isthmo-tectal network (Wang et al., 2006; Marín et al., 2007, 2012; Asadollahi et al., 2011).

Retinal afferents to the GLv have been suggested to be collateral branches of axons that end in the superficial layer of the optic tectum (Cowan et al., 1961; Guiloff et al., 1987; Tombol et al., 2004). Retino-GLv terminals are known to be glutamatergic and, as the retino-tectal endings, endowed with nicotinic receptors (Guo et al., 1998, 2005). Previous physiological work in chick brain slices has shown a nicotinic-dependent presynaptic enhancement of the synaptic transmission between the retinal terminals and the projection cells of the GLv-li (Guo et al., 2005, 2010). Given their cholinergic character, vine-neurons are the most likely candidates to be the source of such modulation, since as we have shown here they end in the GLv-ne homotopically and in close apposition with the retinal terminals. If that were the case, the "centrifugal" effect hypothesized by Ramón y Cajal for the vine-neurons would indeed be carried out, not in the retina, but at the level of the retino-GLv terminals. Interestingly, physiological studies have also shown that the activation of nicotinic receptors enhance GABA release in the GLv-ne and muscarinic receptors inhibits the synaptic retino-GLv transmission (Guo and Chiappinelli, 2002; Guo et al., 2010). Thus, a complex mechanism of excitatory and inhibitory cholinergic effects seems to be taking place in the GLv-ne. We suggest that tectal afferents could be acting upon the GLv projection cells in two ways: excitatory, through the gating of the retinal terminals that drive these cells, and inhibitory, through nicotinic and muscarinic receptors possibly located at the GABAergic intrinsic cells and the projecting cells, respectively (or in a yet unknown element). Taken together, in a scenario in which several GLv loci were simultaneously active by independent visual stimuli, the concurrence of tectal activity upon a given retinal-activated GLv locus could selectively enhance the activity of such a locus (as proposed in figure 14), depressing, at the same time, via

GABAergic enhancement, the activity of the neighboring loci.

Avian and mammalian GLv complex

A common feature of the visual system in amniotes is the presence of a set of retinorecipient structures located adjacent to the lateral wall of the ventral thalamus that could be recognized as a "ventrothalamic complex." These structures have in common an absence of subsequent projections to the telencephalon, together with descendent efferents directed towards pretectal, tegmental, and pontine targets (Butler and Hodos, 2005). In mammals, this ventrothalamic complex is called the GLv complex (in primates pregeniculate nucleus) and is composed of several subnuclei or subdivisions, clustered in a large structure containing two or more retinorecipient neuropils and several nuclear layers (Conley and Friederich-Ecsy, 1993a; Harrington, 1997). A main characteristic of this complex is the presence of retinal, collicular, cortical, and cerebellar afferents (Conley and Friederich-Ecsy, 1993b). In turn, projections from this complex to the medial pons, along with projections to the optic tectum, the zona incerta and other hypothalamic targets, the pretectum, the accessory optic nuclei, and the motor tegmentum, have been confirmed in a number of mammalian species (Harrington, 1997).

In birds, the GLv is also part of a complex constituting a collection of several distinct structures that succeed each other in a rostrocaudal order. Following the nomenclature of Karten and Hodos (1967), this complex includes the nucleus LA, IGL, VLT, and GLv. The literature regarding these nuclei is scant and somewhat confusing; thus, the anatomical and functional reasons to group these structures together are at present unclear. It can be said, however, that the overall pattern of connections of this complex is remarkably similar to that of the mammalian GLv complex. Interestingly, none of the single components of this group exhibit a pattern of connections as diverse as the one attributed to the mammalian complex. The most conspicuous and better known member of the avian ventrothalamic complex, the GLv, lacks of cerebellar afferents, and does not emit a significant topographic projection to the tectum or to the accessory optic nuclei (unpubl. obs.).

A collicular projection upon the GLv complex has been described in many mammalian species such as the cat, the rat, and the tree shrew (Graham, 1977; Cosenza and Moore, 1984; Taylor et al., 1986; Conley and Friederich-Ecsy, 1993b). This projection terminates in the external-most neuropil of the complex (thus, a putative homolog for the GLv-ne in birds) and, as in the avian projection, it follows a topographic arrangement. The cells forming this projection are located in the retinorecipient tectal zone, SGS, without a clear layer arrangement. Unfortunately, the labeling of these cells does not show a fine detailed morphology of dendrites and axons, making it difficult to establish any clear comparison with the vine-neurons described in this study. Moreover, the neurochemical identity of these collicular cells is far from resolved. Therefore, more detailed surveys regarding the morphology and neurochemistry of the tectal cells projecting to the GLv in mammals will be necessary in order to establish a consistent comparative approach. In any case, the avian GLv nucleus should not be considered homologous to the mammalian GLv complex as a whole. To be more specific, we propose to rename the avian GLv nucleus the "nucleus geniculatus lateralis, pars ventralis principalis" (GLv-pri).

SUMMARY

We used tracer and immunohistochemical techniques to characterize the morphology, projection pattern, and neurochemical identity of the neurons that give rise to the TeO-GLv projection. Our data indicate that these neurons project to the GLv. Furthermore, the ChAT immunoreactivity of these cells strongly suggests that the TeO-GLv synapses are cholinergic. Nevertheless, other neurotransmitters involvement cannot be ruled out. The information presented will be valuable for future physiological studies regarding the visual role of the GLv and of the TeO-GLv connection.

ACKNOWLEDGMENTS

We thank Birgit Seibel, Yvonne Schwarz, Gaby Schwabedissen, Agnieszka Brzozowska-Prechtl, Elisa Sentis, and Solano Henriquez for excellent technical assistance; Sebastián Tapia Pino for experimental help; Dr. Camilo Libedinsky for critically reading the article; Dr. Prasad Vaddepalli for microscopy assistance; and Máximo Fernández, Dr. Cristián Gutiérrez and Quirin Krabichler for helpful comments during the conduct of this research.

CONFLICT OF INTEREST

The authors declare no conflict of interest.

AUTHOR CONTRIBUTIONS

All authors had full access to all data in the study and take responsibility for the integrity of the data and the accuracy of the data analysis. Study concept and design: TVZ, HL, JM, HJK, GM. Acquisition of data: TVZ, JM, HJK, GM, SH. Analysis and interpretation of data: TVZ, HL, JM, HJK, GM, SH. Drafting of the article: TVZ,

HL, JM, HJK, GM. Critical revision of the article for important intellectual content: HL, JM, HJK, GM. Statistical analysis: TVZ. Administrative, technical, and material support: HL, JM, HJK, GM.

LITERATURE CITED

Angaut P, Repérant J. 1976. Fine structure of the optic fibre termination layers in the pigeon optic tectum: a Golgi and electron microscope study. Neuroscience 1:93–105.

Asadollahi A, Mysore SP, Knudsen EI. 2011. Rules of competitive stimulus selection in a cholinergic isthmic nucleus of the owl midbrain. J Neurosci 31:6088–6097.

Atoji Y. 2011. Immunohistochemical localization of vesicular glutamate transporter 2 (vGluT2) in the central nervous system of the pigeon (Columba livia). J Comp Neurol 519:2887–2905.

Bagnoli P, Fontanesi G, Alesci R, Erichsen JT. 1992. Distribution of neuropeptide Y, substance P, and Choline acetyltransferase in the developing visual system of the pigeon and effects of unilateral retina removal. J Comp Neurol 318:392–414.

Batista SS, Pires RS, Britto LR. 2002. Differential expression of AMPA-type glutamate receptor subunits during development of the chick optic tectum. Braz J Med Biol Res 35:973–978.

Benowitz LI, Karten HJ. 1976. Organization of the tectofugal visual pathway in the pigeon: a retrograde transport study. J Comp Neurol 167:503–520.

Berger SB, Romero X, Ma C, Wang G, Faubion WA, Liao G, Compeer E, Keszei M, Rameh L, Wang N, Boes M, Regueiro JR, Reinecker H-C, Terhorst C. 2010. SLAM is a microbial sensor that regulates bacterial phagosome functions in macrophages. Nat Immunol 11:920–927.

Bonanno G, Raiteri M. 1987. Presence of a gamma-aminobutyric acid (GABA) uptake system on cholinergic terminals of rat hippocampus: evidence for neuronal coexistence of acetylcholine and GABA? J Pharmacol Exp Ther 240:294–297.

Britto LRG, Keyser KT, Lindstrom JM, Karten HJ. 1992. Immunohistochemical localization of nicotinic acetylcholine receptor subunits in the mesencephalon and diencephalon of the chick (Gallus gallus). J Comp Neurol 317:325–340.

Britto LRG, Torrao AS, Hamassaki-Britto DE, Mpodozis J, Keyser KT, Lindstrom JM, Karten HJ. 1994. Effects of retinal lesions upon the distribution of nicotinic acetylcholine receptor subunits in the chick visual system. J Comp Neurol 350:473–484.

Butler AB, Hodos W. 2005. Comparative vertebrate neuroanatomy: evolution and adaptation. Hoboken, NJ: John Wiley & Sons.

Cheramy A, Leviel V, Glowinski J. 1981. Dendritic release of dopamine in the substantia nigra. Nature 289:537–543.

Conley M, Friederich-Ecsy B. 1993a. Functional organization of the ventral lateral geniculate complex of the tree shrew (Tupaia belangeri). I. Nuclear subdivisions and retinal projections. J Comp Neurol 328:1–20.

Conley M, Friederich-Ecsy B. 1993b. Functional organization of the ventral lateral geniculate complex of the tree shrew (Tupaia belangeri). II. Connections with the cortex, thalamus, and brainstem. J Comp Neurol 328:21–42.

Cosenza RM, Moore RY. 1984. Afferent connections of the ventral lateral geniculate nucleus in the rat: an HRP study. Brain Res 310:367–370.

Cowan WM, Adamson L, Powell TP. 1961. An experimental study of the avian visual system. J Anat 95:545–563.

Crossland WJ, Hughes CP. 1978. Observations on the afferent and efferent connections of the avian isthmo-optic nucleus. Brain Res 145:239–256.

Crossland WJ, Uchwat CJ. 1979. Topographic projections of the retina and optic tectum upon the ventral lateral geniculate nucleus in the chick. J Comp Neurol 185:87–106.

Davidoff MS, Schulze W. 1988. Coexistence of GABA-and choline acetyltransferase (ChAT)-like immunoreactivity in the hypoglossal nucleus of the rat. Histochemistry 89: 25–33.

Dávila JC, Andreu MJ, Real MA, Puelles L, Guirado S. 2002. Mesencephalic and diencephalic afferent connections to the thalamic nucleus rotundus in the lizard, Psammodromus algirus. Eur J Neurosci 16:267–282.

Fritzsch B. 1993. Fast axonal diffusion of 3000 molecular weight dextran amines. J Neurosci Methods 50:95–103.

Gaillard F, Bonfield S, Gilmour GS, Kuny S, Mema SC, Martin BT, Smale L, Crowder N, Stell WK, Sauvé Y. 2008. Retinal anatomy and visual performance in a diurnal cone-rich laboratory rodent, the Nile grass rat (Arvicanthis niloticus). J Comp Neurol 510:525–538.

Gamlin PDR, Cohen DH. 1988. Projections of the retinorecipient pretectal nuclei in the pigeon (Columba livia). J Comp Neurol 269:18–46.

Gioanni H, Palacios A, Sansonetti A, Varela F. 1991. Role of the nucleus geniculatus lateralis ventralis (GLv) in the optokinetic reflex: a lesion study in the pigeon. Exp Brain Res 86:601–607.

Graham J. 1977. An autoradiographic study of the efferent connections of the superior colliculus in the cat. J Comp Neurol 173:629–654.

Guiloff GD. 1991. Ultrastructural study of the avian ventral lateral geniculate nucleus. Vis Neurosci 6:119–134.

Guiloff GD, Maturana HR, Varela FJ. 1987. Cytoarchitecture of the avian ventral lateral geniculate nucleus. J Comp Neurol 264:509–526.

Güntürkün O, Karten HJ. 1991. An immunocytochemical analysis of the lateral geniculate complex in the pigeon (Columba livia). J Comp Neurol 314:721–749.

Guo JZ, Chiappinelli VA. 2002. A novel choline-sensitive nicotinic receptor subtype that mediates enhanced GABA release in the chick ventral lateral geniculate nucleus. Neuroscience 110:505–513.

Guo JZ, Tredway TL, Chiappinelli VA. 1998. Glutamate and GABA release are enhanced by different subtypes of presynaptic nicotinic receptors in the lateral geniculate nucleus. J Neurosci 18:1963–1969.

Guo JZ, Liu Y, Sorenson EM, Chiappinelli VA. 2005. Synaptically released and exogenous ACh activates different nicotinic receptors to enhance evoked glutamatergic transmission in the lateral geniculate nucleus. J Neurophysiol 94:2549–2560.

Guo JZ, Sorenson EM, Chiappinelli VA. 2010. Cholinergic modulation of non-N-methyl-d-aspartic acid glutamatergic transmission in the chick ventral lateral geniculate nucleus. Neuroscience 166:604–614.

Harrington ME. 1997. The ventral lateral geniculate nucleus and the intergeniculate leaflet: interrelated structures in the visual and circadian systems. Neurosci Biobehav Rev 21:705–727.

Hayes BP, Webster KE. 1975. An electron microscope study of the retino-receptive layers of the pigeon optic tectum. J Comp Neurol 162:447–465.

Hellmann B, Güntürkün O, Manns M. 2004. Tectal mosaic: organization of the descending tectal projections in comparison to the ascending tectofugal pathway in the pigeon. J Comp Neurol 472:395–410.

Henke H, Schenker T, Cuénod M. 1976. Effects of retinal ablation on uptake of glutamate, glycine, GABA, proline and choline in pigeon tectum. J Neurochem 26:131–139.

Hoshi H, Tian L-M, Massey SC, Mills SL. 2011. Two distinct types of ON directionally selective ganglion cells in the rabbit retina. J Comp Neurol 519:2509–2521.

Hu M, Naito J, Chen Y, Ohmori Y, Fukuta K. 2004. Afferent and efferent connections of the nucleus geniculatus lateralis ventralis demonstrated by WGA-HRP in the chick. Anat Histol Embryol 33:192–195.

Hunt SP, Künzle H. 1976a. Observations on the projections and intrinsic organization of the pigeon optic tectum: an autoradiographic study based on anterograde and retrograde, axonal and dendritic flow. J Comp Neurol 170: 153–172.

Hunt SP, Künzle H. 1976b. Selective uptake and transport of label within three identified neuronal systems after injection of 3H-GABA into the pigeon optic tectum: an autoradiographic and Golgi study. J Comp Neurol 170:173–189.

Isaacson JS. 2001. Mechanisms governing dendritic ã-aminobutyric acid (GABA) release in the rat olfactory bulb. Proc Natl Acad Sci U S A 98:337–342.

Karten HJ, Hodos W. 1967. A stereotaxic atlas of the brain of the pigeon (Columba livia). Baltimore: Johns Hopkins Press.

Karten HJ, Hodos W, Nauta WJH, Revzin AM. 1973. Neural connections of the "visual wulst" of the avian telencephalon. Experimental studies in the pigeon (Columba livia) and owl (Speotyto cunicularia). J Comp Neurol 150:253–277.

Karten HJ, Cox K, Mpodozis J. 1997. Two distinct populations of tectal neurons have unique connections within the retinotectorotundal pathway of the pigeon (Columba livia). J Comp Neurol 387:449–465.

Ludwig M, Pittman QJ. 2003. Talking back: dendritic neurotransmitter release. Trends Neurosci 26:255–261.

Luksch H, Cox K, Karten HJ. 1998. Bottlebrush dendritic endings and large dendritic fields: motion-detecting neurons in the tectofugal pathway. J Comp Neurol 396:399–414.

Major DE, Luksch H, Karten HJ. 2000. Bottlebrush dendritic endings and large dendritic fields: motion-detecting neurons in the mammalian tectum. J Comp Neurol 423:243–260.

Marín G, Henny P, Letelier JC, Sentis E, Karten H, Mrosko B, Mpodozis J. 2001. A simple method to microinject solid neural tracers into deep structures of the brain. J Neurosci Methods 106:121–129.

Marín G, Salas C, Sentis E, Rojas X, Letelier JC, Mpodozis J. 2007. A cholinergic gating mechanism controlled by competitive interactions in the optic tectum of the pigeon. J Neurosci 27:8112–8121.

Marín G, Durán E, Morales C, González-Cabrera C, Sentis E, Mpodozis J, Letelier JC. 2012. Attentional capture? Synchronized feedback signals from the isthmi boost retinal signals to higher visual areas. J Neurosci 32:1110–1122.

Maturana HR, Varela FJ. 1982. Color-opponent responses in the avian lateral geniculate: a study in the quail (Coturnix coturnix japonica). Brain Res 247:227–241.

Medina L, Reiner A. 1994. Distribution of choline acetyltransferase immunoreactivity in the pigeon brain. J Comp Neurol 342:497–537.

Morino P, Bahro M, Cuénod M, Streit P. 1991. Glutamate-like immunoreactivity in the pigeon optic tectum and effects of retinal ablation. Eur J Neurosci 3:366–378.

Mpodozis J, Letelier J-C, Concha ML, Maturana H. 1995. Conduction velocity groups in the retino-tectal and retino-thalamic visual pathways of the pigeon (Columba livia). Int J Neurosci 81:123–136.

Mpodozis J, Cox K, Shimizu T, Bischof H-J, Woodson W, Karten HJ. 1996. GABAergic inputs to the nucleus rotundus (pulvinar inferior) of the pigeon (Columba livia). J Comp Neurol 374:204–222.

Pateromichelakis S. 1979. Response properties of units in the lateral geniculate nucleus of the domestic chick (Gallus domesticus). Brain Res 167:281–296.

Pérez SE, Yáñez J, Marín O, Anadón R, González A, Rodríguez-Moldes I. 2000. Distribution of choline acetyltransferase (ChAT) immunoreactivity in the brain of the adult trout and tract-tracing observations on the connections of the nuclei of the isthmus. J Comp Neurol 428:450–474.

Pires RS, Britto LR. 1997. Distribution of AMPA-type glutamate receptor subunits in the chick visual system. Braz J Med Biol Res 30:73–77.

Ramón y Cajal S. 1995. Histology of the nervous system. Oxford, UK: Oxford University Press.

Reiner A. 1994. Laminar distribution of the cells of origin of ascending and descending tectofugal pathways in turtles: implications for the evolution of tectal lamination. Brain Behav Evol 43:274–283.

Reiner A, Karten HJ. 1982. Laminar distribution of the cells of origin of the descending tectofugal pathways in the pigeon (Columba livia). J Comp Neurol 204: 165–187.

Reiner A, Veenman CL, Medina L, Jiao Y, Del Mar N, Honig MG. 2000. Pathway tracing using biotinylated dextran amines. J Neurosci Methods 103:23–37.

Repérant J, Ward R, Miceli D, Rio J, Médina M, Kenigfest N, Vesselkin N. 2006. The centrifugal visual system of vertebrates: a comparative analysis of its functional anatomical organization. Brain Res Rev 52:1–57.

Sebestény T, Davies DC, Zayats N, Németh A, Tömböl T. 2002. The ramification and connections of retinal fibres in layer 7 of the domestic chick optic tectum: a Golgi impregnation, anterograde tracer and GABA-immunogold study. J Anat 200:169–183.

Sevigny CP, Bassi J, Williams DA, Anderson CR, Thomas WG, Allen AM. 2012. Efferent projections of C3 adrenergic neurons in the rat central nervous system. J Comp Neurol 520:2352–2368.

Sorenson EM, Parkinson D, Dahl JL, Chiappinelli VA. 1989. Immunohistochemical localization of choline acetyltransferase in the chicken mesencephalon. J Comp Neurol 281:641–657.

Sun Z, Wang H, Laverghetta A, Yamamoto K, Reiner A. 2005. The distribution and cellular localization of glutamic acid decarboxylase-65 (GAD65) mRNA in the forebrain and midbrain of domestic chick. J Chem Neuroanat 29:265–281.

Taylor AM, Jeffery G, Lieberman AR. 1986. Subcortical afferent and efferent connections of the superior colliculus in the rat and comparisons between albino and pigmented strains. Exp Brain Res 62:131–142.

Theiss C, Hellmann B, Güntürkün O. 1998. The differential distribution of AMPA-receptor subunits in the tectofugal system of the pigeon. Brain Res 785:114–128.

Tombol T, Eyre M, Zayats N, Nemeth A. 2004. The internal structure of the nucleus geniculatus lateralis ventralis in the avian brain: a Golgi study and electron microscopic investigation. Cells Tissues Organs 177:237–256.

Vanegas H. 1984. Comparative neurology of the optic tectum. New York: Plenum Press.

Veenman CL, Reiner A. 1994. The distribution of GABA-containing perikarya, fibers, and terminals in the

forebrain and midbrain of pigeons, with particular reference to the basal ganglia and its projection targets. J Comp Neurol 339:209–250.

Veenman CL, Albin RL, Richfield EK, Reiner A. 1994. Distributions of GABAA, GABAB, and benzodiazepine receptors in the forebrain and midbrain of pigeons. J Comp Neurol 344:161–189.

Wang Y, Luksch H, Brecha NC, Karten HJ. 2006. Columnar projections from the cholinergic nucleus isthmi to the optic tectum in chicks (Gallus gallus). A possible substrate for synchronizing tectal channels. J Comp Neurol 494:7–35.

Wylie DR, Gutierrez-Ibanez C, Pakan JM, Iwaniuk AN. 2009. The optic tectum of birds: mapping our way to understanding visual processing. Can J Exp Psychol 63:328–338.